

## Analysis of the effect of lens shutter on image motion in aerial camera

YU Chun-feng, CHEN Zhi-chao, JIA Ping, WANG Nai-xiang, HOU Han

Citation:

YU Chun-feng, CHEN Zhi-chao, JIA Ping, WANG Nai-xiang, HOU Han. Analysis of the effect of lens shutter on image motion in aerial camera[J]. *Chinese Optics*, 2020, 13(3): 616–626. doi: 10.3788/CO.2019-0127

于春风, 陈志超, 贾平, 王乃详, 候汉. 航空相机镜间快门对像移的影响分析[J]. *中国光学*, 2020, 13(3): 616–626. doi: 10.3788/CO.2019-0127

View online: <https://doi.org/10.3788/CO.2019-0127>

---

### Articles you may be interested in

[Rail defect monitoring based on laser Doppler frequency shift theory](#)

基于激光多普勒频移的钢轨缺陷监测

*Chinese Optics*. 2018, 11(6): 991 <https://doi.org/10.3788/CO.20181106.0991>

[Review of image enhancement algorithms](#)

图像增强算法综述

*Chinese Optics*. 2017, 10(4): 438 <https://doi.org/10.3788/CO.20171004.0438>

[Hyperspectral image compression sensing based on dynamic measurement](#)

动态测量的高光谱图像压缩感知

*Chinese Optics*. 2018, 11(4): 550 <https://doi.org/10.3788/CO.20181104.0550>

[Optical/algorithmic co-design of large-field high-quality simple optical system](#)

大视场高像质简单光学系统的光学-算法协同设计

*Chinese Optics*. 2019, 12(5): 1090 <https://doi.org/10.3788/CO.20191205.1090>

[Image restoration approach based on structure dictionary learning](#)

基于结构字典学习的图像复原方法

*Chinese Optics*. 2017, 10(2): 207 <https://doi.org/10.3788/CO.20171002.0207>

[A fiber optic gyro error compensation method based on wavelet neural network](#)

基于小波神经网络的光纤陀螺误差补偿方法

*Chinese Optics*. 2018, 11(6): 1024 <https://doi.org/10.3788/CO.20181106.1024>

## Analysis of the effect of lens shutter on image motion in aerial camera

YU Chun-feng<sup>1,2\*</sup>, CHEN Zhi-chao<sup>1,2</sup>, JIA Ping<sup>1,2</sup>, WANG Nai-xiang<sup>1,2</sup>, HOU Han<sup>1,2</sup>

(1. Changchun Institute of Optics, Fine Mechanics and Physics, Chinese Academy of Sciences, Changchun 130033, China;

2. Key Laboratory of Airborne Optical Imaging and Measurement, Chinese Academy of Sciences, Changchun 130033, China)

\* Corresponding author, E-mail: hou791016@163.com

**Abstract:** In order to improve the photographic resolution of aerial remote sensing cameras and obtain high-resolution aerial images, besides optical system with high modulation transfer function and high-quality imaging medium, the exposure time of shutter should be controlled correctly to ensure that the detector can obtain an appropriate image motion value. Based on the structure and working principle of the lens shutter of an aerial mapping camera, we establish the matrix relationship between the ground object and the image through coordinate transformation method, that is, the relationship between the exposure time of the shutter and the image motion value is determined. The image motion value and residual error of the image motion are analyzed by combining the parameters of the camera speed-height ratio and the pixel size. According to the different installation modes of the aerial camera, when the residual error of the image motion value is more than 1/3 of a pixel in size, the Image Motion Compensation (IMC) mechanism is necessary to the imaging system. Thus a theoretical basis for the design of the IMC mechanism in an aerial camera is provided. The analysis is validated by a static test and flight test. The test results show that the aerial camera clearly captures images and the spatial resolution of its images reaches 36.8 lp/mm, which meets the requirements of our technical index.

**Key words:** lens shutter; image motion; exposure time; residual error of image motion; Image Motion Compensation (IMC)

## 航空相机镜间快门对像移的影响分析

于春风<sup>1,2\*</sup>, 陈志超<sup>1,2</sup>, 贾平<sup>1,2</sup>, 王乃详<sup>1,2</sup>, 侯汉<sup>1,2</sup>

(1. 中国科学院长春光学精密机械与物理研究所 吉林 长春 130033;

2. 中国科学院航空光学成像与测量重点实验室 吉林 长春 130033)

**摘要:** 为了提高航空遥感相机的摄影分辨率, 获得高分辨率的航空图像, 除了采用具有高传递函数的光学系统和高质量

收稿日期: 2019-06-18; 修订日期: 2019-06-28

基金项目: 国家重点研发计划资助项目(No. 2016YFC0803000)

Supported by National Key R&D Program Funding Projects(No. 2016YFC0803000)

成像介质外,还要正确控制快门的曝光时间,以保证探测器能够获得合适的像移量。本文基于一种航空测绘相机镜间快门的结构形式及工作原理,以笛卡尔理论为基础,通过坐标变换方法,建立地面目标和影像之间的矩阵关系,从而确定快门曝光时间和像移量的关系,接着,结合相机速高比、像元尺寸等参数,对像移量及像移残差进行分析。根据相机的不同安装方式,以像移残差为1/3像元尺寸为标准,判定成像系统是否加入像移补偿机构,为相机设计提供理论依据。通过静态测试及飞行试验对分析进行验证。试验结果表明,相机分辨力达到36.8 lp/mm,航拍图像良好,满足指标要求。

**关键词:** 镜间快门;像移量;曝光时间;像移残差;像移补偿

**中图分类号:** TP73      **文献标志码:** A      **doi:** 10.3788/CO.2019-0127

## 1 Introduction

The biggest difference between aerial remote sensing photography and ground photography is that the aerial remote sensor is always in motion during the photography process, which results in the change of the axis of sight of the remote sensor. For a given exposure time, the relative movement between the photographed scene image and the detector will cause image motion<sup>[1]</sup>. The degree of image motion determines the ability of image to distinguish details. Therefore, reducing the image shift can improve the image resolution<sup>[2]</sup>.

In the 1980s, the minimum exposure time of the lens shutter produced by Vinton UK was 3/1 000 s; The KC-6A mapping aerial photography camera produced by Fairchild USA is equipped with a Rapi-dyne lens shutter and has an exposure time range of 1/100~1/1 000 s. The shutter of China's aerospace cameras was developed relatively late. After years of efforts, the exposure time range of the focal plane shutter applied to Hangjia series aerial cameras reached 1/800~1/1 600 s in the 1980 s.

The shutter of an aerial camera must satisfy both the required image density and the necessary quality factor of the sensor in the whole image field<sup>[3]</sup>. Otherwise, the image motion value will be larger than its allowable value. The current method of mechanical Image Motion Compensation (IMC) and optical IMC can't completely compensate for the image motion value of each point in the image<sup>[4]</sup>.

When the lens shutter opens aperture bars for exposure imaging, the image motion will result in a decrease in the dynamic spatial resolution of the camera, which will seriously cause image blurring and tailing. In order to obtain a clear and accurate image, it is necessary to also study the factors that affect the size and direction of image motion value<sup>[5]</sup>.

## 2 Structural design of lens shutter

Combining the technical requirements of the camera with the working characteristics of the shutter, an airborne lens shutter mechanism was developed, which has wide exposure time, adjustment range and high shutter efficiency to ensure that the camera can obtain high-resolution and clear images<sup>[6]</sup>. The shutter is mainly composed of a fast blade, a slow blade, a shutter shell, a transmission gear train and a drive motor. The shutter object is shown in Fig.1. By controlling the rotation of the blade, the shutter exposes the aperture of the fast blade and the slow blade simultaneously. The fast blade controls the exposure time, and the slow blade controls the exposure period, which is equivalent to the shutter speed<sup>[7-9]</sup>.

Assuming the brightness of the target is uniform and unchanged, the aperture area changes with time instead of light flux. As shown in Fig.2, during the shutter operation period, the area of the light-through aperture changes. Point *O* is the origin of the coordinate system, which is the axis of blade rotation. *R* is the radius of the light-through aperture.



Fig. 1 Photograph of shutter

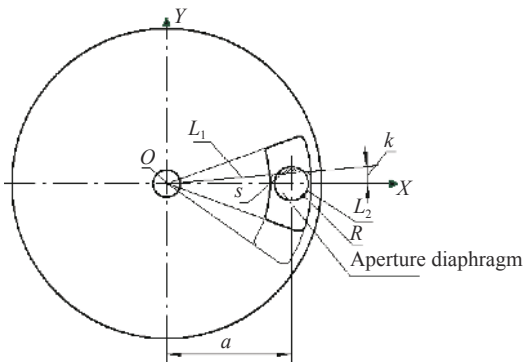


Fig. 2 Schematic diagram of blade scanning aperture

### 3 Analysis of image motion in different camera installation modes

#### 3.1 Analysis of image motion in camera mounted vertically

When the camera is mounted vertically, its axis of sight is perpendicular to the ground. As shown in Fig.3, the camera flies forward at speed  $v$ , the solid line is the position of the image plane at the beginning of the exposure controlled by the shutter and the dotted line is the position of the image plane at the end of the exposure. At the beginning of the exposure, the ground object point  $A$  is transformed into conjugate image point  $A_1$  on the image plane by the optical system. After the time of exposure  $t$  passes, the image plane moves to the dotted line, and the image point  $A_1$  moves to point  $A_2$ . At this time, the ground object point  $A$  appears on the conjugate image at point  $B$  on the image plane. There-

fore, during the time of exposure, the image of the object point  $A$  on the image plane is a straight line segment  $|BA_2|$ , which is the image motion value.

As shown in Fig.3, the geometry of the vector is as follows:

$$\delta = |DA_1| - |MB| = \frac{f}{H}(|AC| - |AN|) = \frac{f}{H}vt. \quad (1)$$

The image motion velocity  $v_i$  is as follows:

$$v_i = \frac{d\delta}{dt} = \frac{f}{H}v, \quad (2)$$

where  $v$  is image motion velocity;  $f$  is length of the focus;  $H$  is attitude of the plane;  $t$  is the real exposure time.

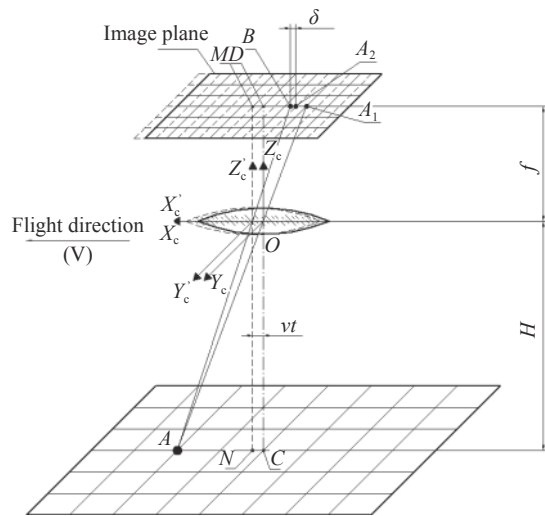


Fig. 3 Forward image shift in camera mounted vertically

When the lens shutter opens the aperture bar, the whole image plane receives light energy at the same time, this means that the exposure time of each point on the image plane is exactly the same. Thus, it is obvious that the scale of any image point on the vertical mounted camera image plane is the same and the image motion value is equal, as shown in Fig.4.

Usually, when the camera receives speed and attitude provided by the aircraft, the two parameters are converted into one parameter for an IMC calculation, so formula (1) is converted into the follow-

ing formula<sup>[10]</sup>:

$$\delta = f\eta t, \quad (3)$$

where  $\eta$  is speed-height ratio.

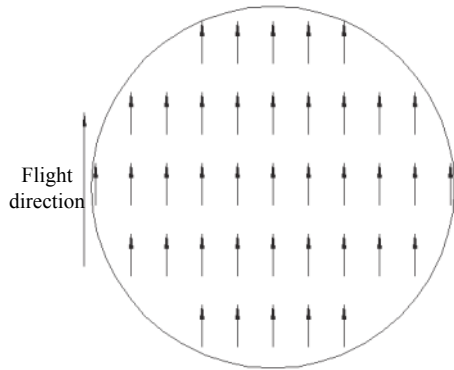


Fig. 4 Image motion vector in camera mounted vertically

In this paper, a digital aerial camera is used for analysis. The focal length of the lens is 56 mm and the pixel size of the CCD detector is  $13 \mu\text{m} \times 13 \mu\text{m}$ . It is believed that image quality is not affected by forward image motion values less than  $1/3$  of a pixel, this means that, the IMC is not needed when the image motion value is less than  $4.3 \mu\text{m}$ . The real range of the speed-height ratio  $\eta$  during flight is  $0.05 \leq \eta \leq 0.17(1/\text{s})$ . When the speed-height ratio changes, the relationship between the exposure time and the image motion value changes accordingly, as shown in Fig.5.

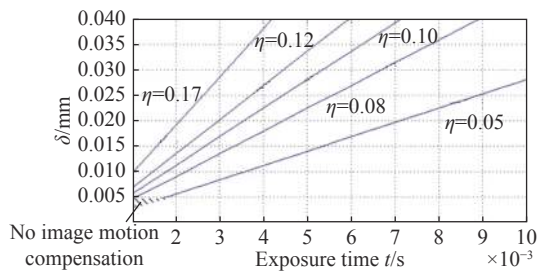


Fig. 5 The relationship between exposure time and image motion value at difference speed-height ratios

It can be seen from Fig.5 that the image motion value increases with exposure time, and the image motion value increases more quickly with a higher speed-height ratio. The limit of the image

motion value is 0.095 mm and the minimum is 0.002 8 mm. When the exposure time is greater than 0.001 4 s or the speed-height ratio is greater than 0.07 rad/s, the IMC mechanism must be applied to reduce image motion. The real range of IMC is  $\pm 1.8^\circ$ , the accuracy is  $0.003^\circ/\text{s}$ . Only when the exposure time is less than 0.001 4 s and the speed-height ratio is between 0.05 rad/s and 0.17 rad/s, it is not necessary to apply the IMC mechanism to reduce the image motion value, as shown in the shaded area.

### 3.2 Analysis of image motion in a camera mounted with some tilt

The camera's forward tilt installation mode is that the camera coordinate system ( $s_c$ ) rotates clockwise around the plane's transverse axis relative to the body coordinate system ( $s_b$ ), i.e. the intersection point  $E$  and  $M$  of the camera coordinate system ( $s_c$ ) with the ground and image plane moved to points  $C$  and  $N$ . The process of generating forward image motion on the image plane is shown in Fig.6. At the beginning of exposure, the ground object point  $A$  is transformed into the image point  $A_1$  on image plane after transversing through optical system. After exposure time  $t$ , ground object point  $A$  moves to point  $B$  and becomes image point  $A_2$  on the image plane. The short line between image point  $A_1$  and image point  $A_2$  is the image formed by object point  $A$  on the image plane while the aircraft is in motion.  $\delta$  is the image motion value.

It is supposed that the coordinates of the image point  $A_1$  in the image plane coordinate system are  $(x, y, z)$ ,  $z = 0$ . The coordinate system  $s_p$  is translated to the coordinate system  $s_c$  and the coordinates after the counter-clockwise rotation angle  $\beta$  is as follows:

$$\begin{bmatrix} x' \\ y' \\ z' \end{bmatrix} = \begin{bmatrix} 1 & 0 & 0 \\ 0 & \cos\beta & \sin\beta \\ 0 & -\sin\beta & \cos\beta \end{bmatrix} \begin{bmatrix} x \\ y \\ z - f \end{bmatrix}. \quad (4)$$

According to the geometric projection relation of the optical system, it can be seen that object point

A moves to point B after exposure time  $t$ , and the coordinates of point B in the body coordinate system are  $(x'', y'', z'')$ , as follows:

$$\begin{bmatrix} x'' \\ y'' \\ z'' \\ 1 \end{bmatrix} = \begin{bmatrix} H/Z' & 0 & 0 & 0 \\ 0 & H/Z' & 0 & -vt \\ 0 & 0 & H/Z' & 0 \\ 0 & 0 & 0 & 1 \end{bmatrix} \begin{bmatrix} x' \\ y' \\ z' \\ 1 \end{bmatrix}, \quad (5)$$

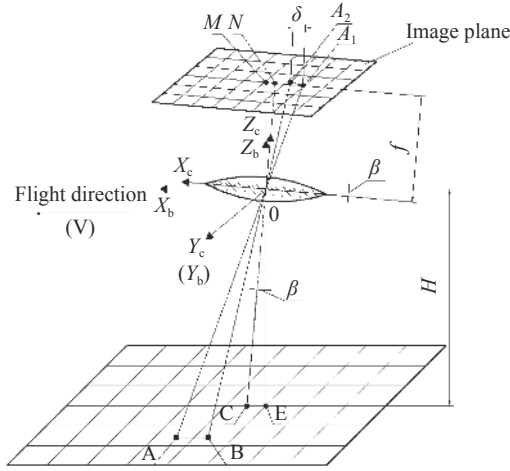


Fig. 6 Image motion in camera mounted tilting forward

The coordinates of the image point corresponding to object point B formed by the optical system in the body coordinate system  $s_b$  are  $(x_1, y_1, z_1)$ . At this time, the scale is  $z_1/H$ , which can be obtained from the geometric relationship of the image:

$$x_1 = x'' \times \frac{z_1}{H} = \frac{x'}{z'} H \times \frac{z_1}{H} = \frac{x' z_1}{z'}, \quad (6)$$

$$y_1 = y'' \times \frac{z_1}{H} = \left( \frac{y'}{z'} H - vt \right) \times \frac{z_1}{H} = \frac{y' z_1}{z'} - \frac{vt z_1}{H}, \quad (7)$$

$$z_1 = z_1. \quad (8)$$

The body coordinate system  $s_b$  coincides with the coordinate system  $s_c$  after the clockwise rotation angle  $\beta$ . The coordinates of the image points in the coordinate system  $s_c$  are  $(x_2, y_2, z_2)$ , as follows:

$$\begin{bmatrix} x_2 \\ y_2 \\ z_2 \end{bmatrix} = \begin{bmatrix} 1 & 0 & 0 \\ 0 & \cos\beta & -\sin\beta \\ 0 & \sin\beta & \cos\beta \end{bmatrix} \begin{bmatrix} x_1 \\ y_1 \\ z_1 \end{bmatrix}. \quad (9)$$

The coordinates  $(x_2, y_2, z_2)$  in the coordinate system  $s_c$  are transformed into those in the image plane coordinate system  $s_p$ . In other words, the coordinate system  $s_c$  is moved negatively by  $f$  along the  $Z_c$  axis, and the coordinates  $(x_3, y_3, z_3)$  after transformation are as follows:

$$x_3 = x_2, \quad (10)$$

$$y_3 = y_2, \quad (11)$$

$$z_3 = z_2 + f. \quad (12)$$

From formula (4)~(12), it can be concluded that both the image plane and the direction of the camera installed in the forward tilt mode will produce image motion, whose values are as follows:

$$\delta_x = \frac{-vt(x \sin\beta + f \cos\beta)^2}{vt \sin\beta(x \sin\beta + f \cos\beta) - Hf}, \quad (13)$$

$$\delta_y = \frac{-yvt \sin\beta(x \sin\beta + f \cos\beta)}{vt \sin\beta(x \sin\beta + f \cos\beta) - Hf}. \quad (14)$$

It can be seen from formula (13) and (14) that the image motion value along the direction of flight is only related to  $x$  of the image plane coordinate system. Also, the image motion value in the vertical flight direction is related to  $x$  and  $y$ , and the image motion follows the flight direction of the the plane  $X_c O Z_c$  and there is no image motion in the vertical direction. For digital aerial cameras, it can be shown from formula (14) that the maximum value of image motion in vertical flight direction is 0.003 7 mm, which is less than 1/3 of the pixel size when the LOS (Line-of-Sight) inclination  $\beta = 3^\circ$ , speed-height ratio  $\eta = 0.17$  and shutter exposure time  $t = 0.01$  s. The image motion mentioned will not affect image quality. Therefore, only the image motion along the flight direction is considered. When the field of view angle is  $0^\circ$ , the image motion value of the central field of view is as follows:

$$\delta_{x0} = \frac{vt f \cos^2\beta}{H - vt \sin\beta \cos\beta}, \quad (15)$$

$$\delta_{y0} = 0 \quad (16)$$

It can be seen from formula (15) that equation (15) is the same as equation (3) when the forward tilt angle of the viewing axis  $\beta$  is  $0^\circ$ . It also can be seen that the vertical installation of the camera is a special case of the forward tilt installation.

The distribution and histogram of image motion vectors in the full field of view on the image plane of the camera installed in a forward tilt mode are shown in Fig. 7. The image plane is  $7\,168 \times 4\,096$ , the pixel and 105 image points are distributed on the image plane for vector analysis. The direction of flight is along the axis with 4 096 pixels. Fig.7 shows the distribution of image motion vectors on the image plane when the speed-height ratio is 0.16 rad/s, the shutter exposure time is 0.01 s, and the forward tilt angle is  $5^\circ$ . All vectors are analyzed by histogram<sup>[11]</sup>.

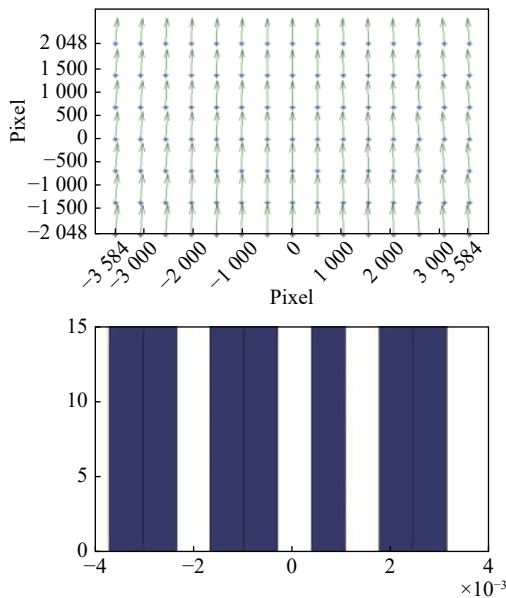


Fig. 7 Schematic and histogram of image motion vector in camera lean mounted forward

The histogram only demonstrates the distribution of image motion along the flight direction. Combining formula (13) and (14), we can see that the maximum image motion value  $\delta_y$ , which is perpendicular to the flight direction, occurs at the max-

imum values of  $x$  and  $y$ , i.e. in the image plane coordinate system  $s_p$ , (24.564,43.008) and (-43.008, 24.564), and the minimum  $\delta_y$  occurs at  $y = 0$ , i.e. in the axis  $x$  of the coordinate system  $s_p$ . The maximum image motion value  $\delta_x$  in the direction of flight occurs at  $x = 24.564$ , and the minimum image motion value  $\delta_x$  occurs at  $x = -24.564$ . In the absence of the influence of the attitude angle of the aircraft, the installation of the camera's forward tilt mode will also result in image motion at different speeds, and the residual error of image motion value is as follows:

$$\delta_{x\Delta} = \frac{vtf\cos^2\beta}{vt\sin\beta\cos\beta-H} - \frac{vt(x\sin\beta+f\cos\beta)^2}{vt\sin\beta(x\sin\beta+f\cos\beta)-Hf} \quad (17)$$

From formula(17), it can be seen that the shutter exposure time is 0.01 s when the speed-height ratio is 0.17 rad/s, and the forward tilt angle is  $3^\circ$ , the maximum forward image motion value along the flight direction is 0.004 49 mm, which is bigger than 1/3 of the pixel in size and therefore can't meet the imaging quality requirements. If the exposure time of the shutter is shortened to meet the requirements of imaging quality, the shortest exposure time should be 1/108 s. Through analysis, the distribution and histogram of image motion value residual vectors in the full field of view on the camera's image plane installed with a forward tilt mode can be obtained, as shown in Fig. 8.

From Fig.8, the residual image motion value of the central field of view is 0 and the larger the field angle, the larger the residual image motion value. The vector of the residual image motion value tends to point to the axis of sight. In addition, the residual image motion value of the whole image plane is distributed symmetrically with respect to the plane  $x_c o z_c$ .

It can be seen from the histogram that the residual image motion value of more than 40 points is greater than 0.004 mm at the edge of the image plane. When the speed-height ratio changes, the relationship between exposure time and the image

motion value changes accordingly, as shown in Fig.9.

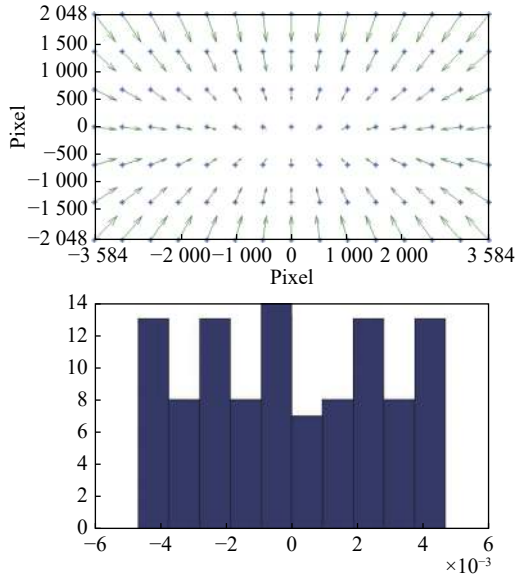


Fig. 8 Schematic and histogram of forward residual image motion in camera mounted leaning forward

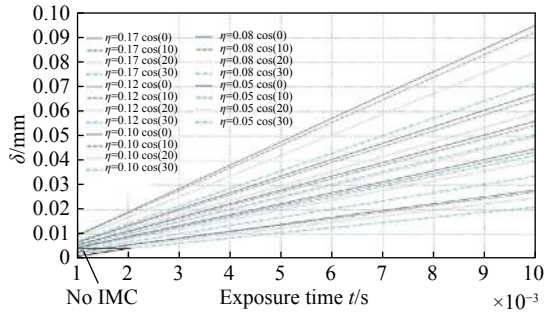


Fig. 9 The relationship between exposure time and image shift at difference V/H and lean angle forward

From Fig.9, with the same shutter exposure time, the forward image motion value of the central field of view decreases gradually with a decrease of the speed-height ratio, while the forward image motion value of the central field of view increases gradually with a decrease in the rake angle  $\beta$ . When the rake angle is  $0^\circ$ , the relationship between image motion and exposure time is the same as when the camera is installed vertically. The maximum exposure time of the shutter between the mirrors in the shadowed area is 0.001 9 s.

### 3.3 Analysis of image motion in an aircraft with attitude changes

The flight attitude of an aircraft changes at any moment and there are three kinds of flight attitude changes, namely pitch, roll and yaw, which are equivalent to the three Euler angle changes between the body coordinate system (camera coordinate system) and the track coordinate system. The process of the ground object's position transformation from the fixed coordinate system on the vertical ground to the image plane coordinate system is shown in Fig.10<sup>[12]</sup>.

It is necessary to analyze the image motion caused by a change in flight attitude to analyze the relationship between the rotation of the track coordinate system and the body coordinate system. The transformation process is as follows:

$$\begin{bmatrix} x_p \\ y_p \\ z_p \\ 1 \end{bmatrix} = \begin{bmatrix} -\frac{f}{H} & 0 & 0 & 0 \\ 0 & -\frac{f}{H} & 0 & 0 \\ 0 & 0 & -\frac{f}{H} & -f \\ 0 & 0 & 0 & 1 \end{bmatrix} \begin{bmatrix} 1 & 0 & 0 & 0 \\ 0 & \cos\varphi & \sin\varphi & 0 \\ 0 & -\sin\varphi & \cos\varphi & 0 \\ 0 & 0 & 0 & 1 \end{bmatrix} \begin{bmatrix} \cos\theta & 0 & \sin\theta & 0 \\ 0 & 1 & 0 & 0 \\ -\sin\theta & 0 & \cos\theta & 0 \\ 0 & 0 & 0 & 1 \end{bmatrix} \begin{bmatrix} x_g \\ y_g \\ z_g \\ 1 \end{bmatrix} \quad (18)$$

$$\begin{bmatrix} \cos\psi & \sin\psi & 0 & 0 \\ -\sin\psi & \cos\psi & 0 & 0 \\ 0 & 0 & 1 & 0 \\ 0 & 0 & 0 & 1 \end{bmatrix} \begin{bmatrix} 1 & 0 & 0 & -vt \\ 0 & 1 & 0 & 0 \\ 0 & 0 & 1 & -H \\ 0 & 0 & 0 & 1 \end{bmatrix} \begin{bmatrix} x_g \\ y_g \\ z_g \\ 1 \end{bmatrix}$$

When the attitude of the plane doesn't change at the initial moment of exposure, the three Euler angles are all 0. The coordinates of the ground ob-

ject points corresponding to  $(x_p, y_p, z_p)$  at any point on the image plane are  $(x_g, y_g, 0)$  in the fixed coordinate system of the vertical ground.



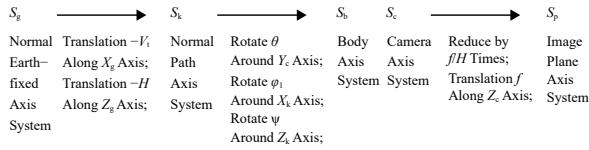


Fig. 10 Diagram of coordinate transformation relation

The relationship between object points and image points can be obtained from geometric optics as follows:

$$x_g = -\frac{H}{f}x_p, y_g = -\frac{H}{f}y_p. \quad (19)$$

After the exposure time  $t$  of the shutter between

$$\begin{bmatrix} x'_p \\ y'_p \\ z'_p \\ 1 \end{bmatrix} = \begin{bmatrix} -\frac{f}{H} \cos \theta \cos \psi & -\frac{f}{H} \cos \theta \sin \psi & -\frac{f}{H} \sin \theta & \frac{f}{H} vt \cos \theta \cos \psi + f \sin \theta \\ \frac{f}{H} (\sin \varphi \sin \theta \cos \psi + \cos \varphi \sin \psi) & \frac{f}{H} (\sin \varphi \sin \theta \sin \psi - \cos \varphi \cos \psi) & -\frac{f}{H} \sin \varphi \cos \theta & -\frac{f}{H} vt (\sin \varphi \sin \theta \cos \psi + \cos \varphi \sin \psi) + f \sin \varphi \cos \theta \\ \frac{f}{H} (\cos \varphi \sin \theta \cos \psi - \sin \varphi \sin \psi) & \frac{f}{H} (\cos \varphi \sin \theta \sin \psi + \sin \varphi \cos \psi) & -\frac{f}{H} \cos \varphi \cos \theta & -\frac{f}{H} vt (\cos \varphi \sin \theta \cos \psi - \sin \varphi \sin \psi) + f \cos \varphi \cos \theta - f \\ 0 & 0 & 0 & 1 \end{bmatrix} \begin{bmatrix} x_g \\ y_g \\ 0 \\ 1 \end{bmatrix}. \quad (20)$$

Substituting equation (19) into the above, we can get:

$$x'_p = \cos \theta \cos \psi x_p + \cos \theta \sin \psi y_p + \frac{f}{H} vt \cos \theta \cos \psi + f \sin \theta, \quad (21)$$

$$y'_p = f \sin \varphi \cos \theta + \cos \varphi \cos \psi y_p - (\sin \varphi \sin \theta \cos \psi + \cos \varphi \sin \psi) x_p - \sin \varphi \sin \theta \sin \psi y_p - \frac{f}{H} vt (\sin \varphi \sin \theta \cos \psi + \cos \varphi \sin \psi), \quad (22)$$

$$z'_p = -(\cos \varphi \sin \theta \cos \psi - \sin \varphi \sin \psi) x_p - (\cos \varphi \sin \theta \sin \psi + \sin \varphi \cos \psi) y_p - \frac{f}{H} vt (\cos \varphi \sin \theta \cos \psi - \sin \varphi \sin \psi) + f \cos \varphi \cos \theta - f, \quad (23)$$

As can be seen from the above analysis, the image motion caused by the flight attitude after shutter exposure time  $t$  occurs along the three axes of

$$\delta_x = x'_p - x_p = \cos \theta \cos \psi x_p + \cos \theta \sin \psi y_p + \frac{f}{H} vt \cos \theta \cos \psi - f \sin \theta - x_p, \quad (24)$$

$$\delta_y = y'_p - y_p = f \sin \varphi \cos \theta + \cos \varphi \cos \psi y_p - (\sin \varphi \sin \theta \cos \psi + \cos \varphi \sin \psi) x_p - \sin \varphi \sin \theta \sin \psi y_p - \frac{f}{H} vt (\sin \varphi \sin \theta \cos \psi + \cos \varphi \sin \psi) - y_p, \quad (25)$$

$$\delta_z = z'_p - z_p = -(\cos \varphi \sin \theta \cos \psi - \sin \varphi \sin \psi) x_p - (\cos \varphi \sin \theta \sin \psi + \sin \varphi \cos \psi) y_p - \frac{f}{H} vt (\cos \varphi \sin \theta \cos \psi - \sin \varphi \sin \psi) + f \cos \varphi \cos \theta - f - z_p. \quad (26)$$

From equation (24), the forward image motion caused by the flight attitude is only related to the speed-height ratio, the focal length of the lens, the pitch angle and the yaw angle, but the roll angle has nothing to do with the forward image motion. When the attitude of aircraft doesn't change, and all three

mirrors passes, the aircraft flies  $vt$  with respect to the ground in the direction of track coordinate system  $X_c$ , that is, the body coordinate system moves  $vt$  with respect to the fixed coordinate system on the vertical ground. Euler angle can be obtained by the angular velocity of the plane multiplied by  $t$ .

At this point, the coordinates  $(x_g, y_g, 0)$  of the ground object points in the fixed coordinate system of vertical ground become the corresponding  $(x'_p, y'_p, z'_p)$  through the optical system in the coordinate system of the image plane. This can be obtained from equation (18).

the image plane coordinate system. The image motion value along the three axes are as follows:

Euler angles are zero, equations (24) and (1) are identical. The magnitude of the image motion value in the three directions is related to  $x_p$  and  $y_p$ . Equation (26) is the amount of defocusing, which is also related to  $z_p$ .

Through an analysis of equations (24) and (25),

it can be seen that image motion is mainly caused by relative motion between the aircraft and the ground, while image motion from other sources is smaller by one order of magnitude. Therefore, as long as the forward image motion is effectively compensated, the effect of image motion on image quality can practically be eliminated. The image motion value of the central field of view is as follows:

$$\delta_{x0} = \frac{f}{H}vt \cos \theta \cos \psi - f \sin \theta, \quad (27)$$

$$\delta_{y0} = f \sin \varphi \cos \theta - \frac{f}{H}vt(\sin \varphi \sin \theta \cos \psi + \cos \varphi \sin \psi). \quad (28)$$

According to equation (27), when both pitch angle and yaw angle are equal to zero, equations (27) and (3) are identical. The image motion vector distribution and histogram on the field of sight of the camera with varying flight attitude is shown in Fig.11. The flight direction occurs along the 4 096 pixel axis. 105 points are uniformly selected on the surface for vector analysis. In Fig.11, these were the points where the speed-height ratio is 0.16 rad/s, the shutter exposure time is 0.01 s and the three Euler angles are 5°.

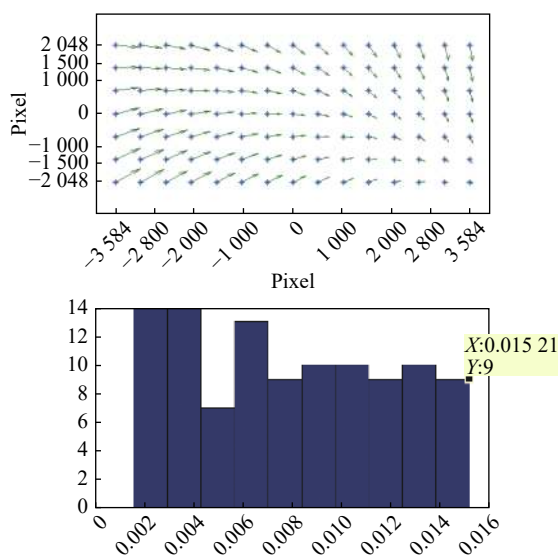


Fig. 11 The schematic and histogram of image shift vectors caused by aircraft attitude changes

The histogram displays the total statistical points whose image motion value is bigger than 0.004 mm reaching 77 on the whole image plane.

## 4 The experiment and analysis

In order to verify the feasibility of this method, an experiment was conducted. The test principle is illustrated in Fig.12.

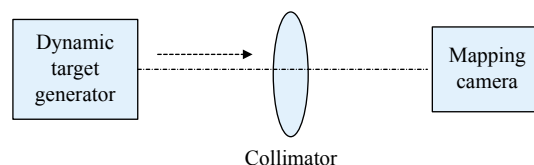


Fig. 12 Schematic diagram of experimental device

The mapping camera was installed in front of the dynamic target generator and the alignment between the visual axis and the target center was adjusted. The image of the dynamic target generator from the camera was used to verify whether its dynamic resolution met the requirements<sup>[13]</sup>.

The experiment device is shown in Fig.13. The imaging CCD detector is an aerial scan CCD with a resolution of 7168×4096, a pixel size of 13 μm×13 μm and a frame rate of 30 frame/s. The focal length of the mapping camera is 56 mm, relative aperture is 1:6 and the operating wavelength is 0.4~0.9 μm. By adjusting the target generator to simulate different speed-height ratios and shutter exposure time, the discrimination rate plate image is obtained, as shown in Fig.14.



Fig. 13 Measuring setup

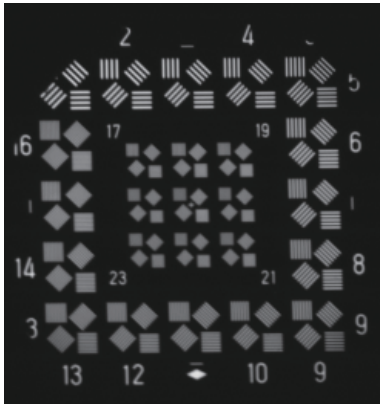


Fig. 14 Photo of the dynamic target

The obtained experimental results are shown in Table 1. The visual resolution of the image can reach 36.8 lp/mm. The image achieves the required precision. In flight experiment test, the image is clear as shown in Fig.15.

Tab. 1 Imaging experiment results

Measurement times	Visual resolution(lp/mm)
1	36.5
2	36.5
3	37.2
4	36.5
5	37.2
Average	36.8



Fig. 15 Radial drone image in flight

The diffraction limit spatial resolution of the optical system is 38.5 lp/mm. The spatial resolution design index of the mapping camera is 34 lp/mm. According to the control precision requirement, the image motion value of the image is less than 1/3 pixel size, which means that the image motion value is less than 4.3  $\mu\text{m}$ . The spatial resolution of the identification plate imaging experiment can reach 36.8 lp/mm, which is close to the diffraction limit resolution and meets the requirements for the technical index.

## 5 Conclusion

Based on requirements for digital aerial mapping cameras, a lens shutter of airborne remote sensors was designed. The influence of the installation mode of a camera on image motion was analyzed. The influence of the aircraft flight attitude on image motion was analyzed. Combined with camera parameters such as speed-height ratio, the relationship between the lens shutter exposure time and the image motion was derived. When there is minimal system signal-to-noise ratio, the short shutter exposure time can reduce the image motion value, which leads to clear images from an aerial camera, which provides a theoretical basis for adding the IMC mechanism. Through experimentation and flight tests, a clear image of the discrimination rate plate and flight target were obtained. The spatial resolution of a flight target image can reach 36.8 lp/mm using this method, which is close to the diffraction limit resolution and meets the requirements of the technical index.

### 参考文献:

- [1] 谢尔巴科夫. 航空照相机的设计与计算[M]. 孙振洲, 周桂琴, 译. 吉林: 吉林省科技翻译协会, 1985. SIERBAKOV. *Design and Calculation of Aerial Camera*[M]. SUN ZH ZH, ZHOU G Q, trans. Jilin: The Association of Science and Technology Translation in Jilin, 1985. (in Chinese)
- [2] 王之卓. 摄影测量原理[M]. 北京: 测绘出版社, 1979. WANG ZH ZH. *Photogrammetry Principle*[M]. Beijing: Surveying and Mapping Press, 1979. (in Chinese)

- [3] 张雷, 丁亚林, 张洪文, 等. 基于正时带的帘幕式快门设计与精度分析[J]. *光学精密工程*, 2013, 21(2): 380-387.  
ZHANG L, DING Y L, ZHANG H W, *et al.*. Design and precision analysis of curtain type shutter based on timing belt[J]. *Optics and Precision Engineering*, 2013, 21(2): 380-387. (in Chinese)
- [4] DURFEE D, JOHNSON W, MCLEOD S. Advanced electro-mechanical micro-shutters for thermal infrared night vision imaging and targeting systems[J]. *Proceedings of SPIE*, 2007, 6452: 65422C.
- [5] 刘明, 刘刚, 李友一, 等. 航空相机的像移计算及其补偿分析[J]. *光电工程*, 2004, 31(S1): 12-14.  
LIU M, LIU G, LI Y Y, *et al.*. The effect of image motion on the quality of aerial camera images[J]. *Opto-Electronic Engineering*, 2004, 31(S1): 12-14. (in Chinese)
- [6] 远国勤. 具有前向像移补偿功能的彩色大面阵测绘相机内方位元素标定研究[D]. 长春: 中国科学院研究生院(长春光学精密机械与物理研究所), 2013.  
YUAN G Q. Research on the calibration of inner orientation elements for area scan color CCD mapping camera with forward image motion compensation mechanism[D]. Changchun: Changchun Institute of Optics, Fine Mechanics and Physics, Chinese Academy of Sciences, 2012. (in Chinese)
- [7] 于春风, 李辉, 贾平, 等. 航空摄影镜间快门机构的设计[J]. *光学精密工程*, 2018, 26(1): 105-113.  
YU CH F, LI H, JIA P, *et al.*. Lens shutter for aerial photography[J]. *Optics and Precision Engineering*, 2018, 26(1): 105-113. (in Chinese)
- [8] 任航, 袁红艳. 面阵CCD航测相机像移补偿技术研究[J]. *半导体光电*, 2011, 32(3): 417-420, 428.  
REN H, YUAN H Y. Research on image motion compensation of airborne camera of focal plane CCD[J]. *Semiconductor Optoelectronics*, 2011, 32(3): 417-420, 428. (in Chinese)
- [9] 于春风. 新型航空镜间快门的研究与光学特性分析[D]. 长春: 中国科学院研究生院(长春光学精密机械与物理研究所), 2013.  
YU CH F. Design and analysis of optical characteristic on new type aerial lens shutter[D]. Changchun: Changchun Institute of Optics, Fine Mechanics and Physics, Chinese Academy of Sciences, 2013. (in Chinese)
- [10] 颜昌翔, 王家骥. 航相机像移补偿计算的坐标变换方法[J]. *光学精密工程*, 2000, 8(3): 203-207.  
YAN CH X, WANG J Q. Method of coordinate transformation for IM&IMC calculation in aerospace camera system[J]. *Optics and Precision Engineering*, 2000, 8(3): 203-207. (in Chinese)
- [11] 陈博洋. 彩色遥感图像的亮度直方图局部线性化增强[J]. *光学精密工程*, 2017, 25(2): 502-508.  
CHEN B Y. Local linear enhancement of luminance histogram of color remote sensing image[J]. *Optics and Precision Engineering*, 2017, 25(2): 502-508. (in Chinese)
- [12] 王家琪, 于平, 颜昌翔, 等. 航天光学遥感器像移速度矢计算数学模型[J]. *光学学报*, 2004, 24(12): 1585-1589.  
WANG J Q, YU P, YAN CH X, *et al.*. Space optical remote sensor image motion velocity vector computational modeling[J]. *Acta Optica Sinica*, 2004, 24(12): 1585-1589. (in Chinese)
- [13] 李刚, 杨名宇. 基于联合变换相关的机载航空相机像移测量[J]. *中国光学*, 2015, 8(3): 401-406.  
LI G, YANG M Y. Image motion measurement for airborne camera based on joint transform correlation[J]. *Chinese Journal of Optics*, 2015, 8(3): 401-406. (in Chinese)

#### Author Biographics:



YU Chun-feng (1979—), was born in Changchun, Jilin province. In 2013, he graduated from University of Chinese Academy of Sciences. Now he is working as an associate professor at Changchun Institute of Optics, Fine Mechanics and Physics, Chinese Academy of Sciences. His research interests are aerial imaging and measurement technology. E-mail: hou791016@163.com